


Article

Influence of the Thickness of Freezing of the Soil Surface and Snow Cover on Methane Emissions during Freezing of Seasonal Permafrost

Chenzheng Li ^{1,*}, Anatoly V. Brouchkov ¹, Viktor G. Cheverev ¹, Andrey V. Sokolov ² and Bicheng Zhou ¹ 

¹ Geology Faculty, Lomonosov Moscow State University, 1 Leninskie Gory, Moscow 119991, Russia; brouchkov@geol.msu.ru (A.V.B.); cheverev44@mail.ru (V.G.C.); zhoubicheng@mail.ru (B.Z.)

² NIIT LLC., 20 Kulakova Str., Moscow 123592, Russia; sok44@yandex.ru

* Correspondence: lichenzheng0912@gmail.com

Abstract: Methane, a type of greenhouse gas, poses considerable concern for humans. This study uses field experiments and satellite measurements to explore methane emission mechanisms during the freezing of seasonal permafrost and the contributing factors. In the transitional seasons of autumn and winter, as soil begins to freeze, methane emissions surge dramatically in a brief period. During this phase, the emissions peak, enabling the soil to accumulate over 9000 mg/m³ of methane rapidly. Snow cover also plays a crucial role in mitigating methane emissions. The porous nature of a sufficiently thick snow cover aids in temporarily trapping methane through a stratified blocking process, effectively matching the inhibitory capability of unfrozen soil. In comparison to unfrozen soil (54–237 mg/m³), snow cover can suppress methane emissions up to 20 times more, reducing emissions by as much as 3399 mg/m³.

Keywords: greenhouse gases; seasonal permafrost; methane emissions; snow cover



Citation: Li, C.; Brouchkov, A.V.; Cheverev, V.G.; Sokolov, A.V.; Zhou, B. Influence of the Thickness of Freezing of the Soil Surface and Snow Cover on Methane Emissions during Freezing of Seasonal Permafrost. *Atmosphere* **2024**, *15*, 1231. <https://doi.org/10.3390/atmos15101231>

Academic Editors: Célia dos Anjos Alves and Caiqing Qin

Received: 4 August 2024

Revised: 1 October 2024

Accepted: 12 October 2024

Published: 15 October 2024



Copyright: © 2024 by the authors. Licensee MDPI, Basel, Switzerland. This article is an open access article distributed under the terms and conditions of the Creative Commons Attribution (CC BY) license (<https://creativecommons.org/licenses/by/4.0/>).

1. Introduction

The concentration of greenhouse gases in the atmosphere is directly and positively correlated with the greenhouse effect. Methane, the second most prevalent greenhouse gas after carbon dioxide, has seen a rapid increase in atmospheric concentrations over the past few decades. Since the pre-industrial era, global atmospheric methane levels have escalated by 150%, rising from 0.715 to 1.813 ppm [1]. Soil carbon in permafrost regions holds approximately twice the atmospheric volume, estimated at nearly 1.6 trillion tons [2,3]. As permafrost thaws, it releases trapped greenhouse gases such as methane and carbon dioxide into the atmosphere [4–7], thereby exacerbating global warming. This release accelerates the sudden thawing of permafrost, significantly disrupting the normal seasonal freezing and thawing processes worldwide [8–11].

Under the influence of global warming, the extent of permafrost is diminishing, leading to projections of increasing methane emissions in the future [12–14]. Seasonal permafrost is also experiencing a shorter duration of freeze and reduced coverage [15,16]. Methane emissions are known to increase during the freezing of the soil surface [17,18]. Some researchers argue that after the soil surface has frozen, the primary factors influencing gas emissions are the bidirectional freezing and the resultant spatial closure caused by both the surface and subsurface frozen layers [19–21].

This article explores methane emissions in the Nakhabino area through a dual approach of field experiments and satellite measurements. The field experiments provide a direct observation of methane emissions, focusing on the mechanisms during the autumn freeze of seasonal permafrost. These experiments reveal that snow cover, alongside soil surface conditions and the subterranean frost layer, plays a crucial role in modulating methane emissions. The findings indicate that increasing snow thickness diminishes the

soil surface freezing process, reducing the methane concentration within the soil by 39–81%, while increasing it at the soil surface by 13–35% and in the air by 18–250%. The satellite measurements corroborate these results, showing a sharp rise in airborne methane levels as the snow depth increases. The interplay of snow cover significantly influences the containment and release of methane. This study offers valuable insights and data for predicting future methane emissions and developing strategies to mitigate them under permafrost conditions.

2. Experimental Site and Method

The experimental site was chosen on the outskirts of Nakhabino in the Moscow region ($55^{\circ}51'44.3''$ N, $37^{\circ}11'21.3''$ E, Figure 1). This site is an open area free from human activities and features sparse vegetation. It is situated in a region with a humid continental climate. The area, characterized by seasonal permafrost, receives abundant snowfall and is composed of Quaternary sediments such as loamy and sandy soils [22]. The soil is underlain by moraine-covered silty loams that can be up to tens of meters thick. The podzolic soil features a dense turf layer that extends down to 20 cm. The upper half-meter of soil is categorized as medium loam, while the deeper layer (50–100 cm) is heavier loam. The bulk density of these soil layers typically ranges between 1.50 and 1.64 g/cm³. According to a century of data from the Timiryazev Academy observatory, the first snowfall usually occurs on 11 October, with snow cover appearing by 3 November and becoming stable by 25 November. Annual precipitation varies between 500 and 650 mm, fostering effective leaching that moves clay particles from upper to lower layers, contributing to the formation of podzolic soil. The water in the soil exhibits a slightly acidic pH. The site is positioned on a watershed—a hilly plateau between the Nakhabinka River and a deep ravine, reaching up to approximately 140 m in elevation. The area supports sparse forest vegetation, predominantly rare birches, and features diverse sedges with a small amount of sphagnum moss.

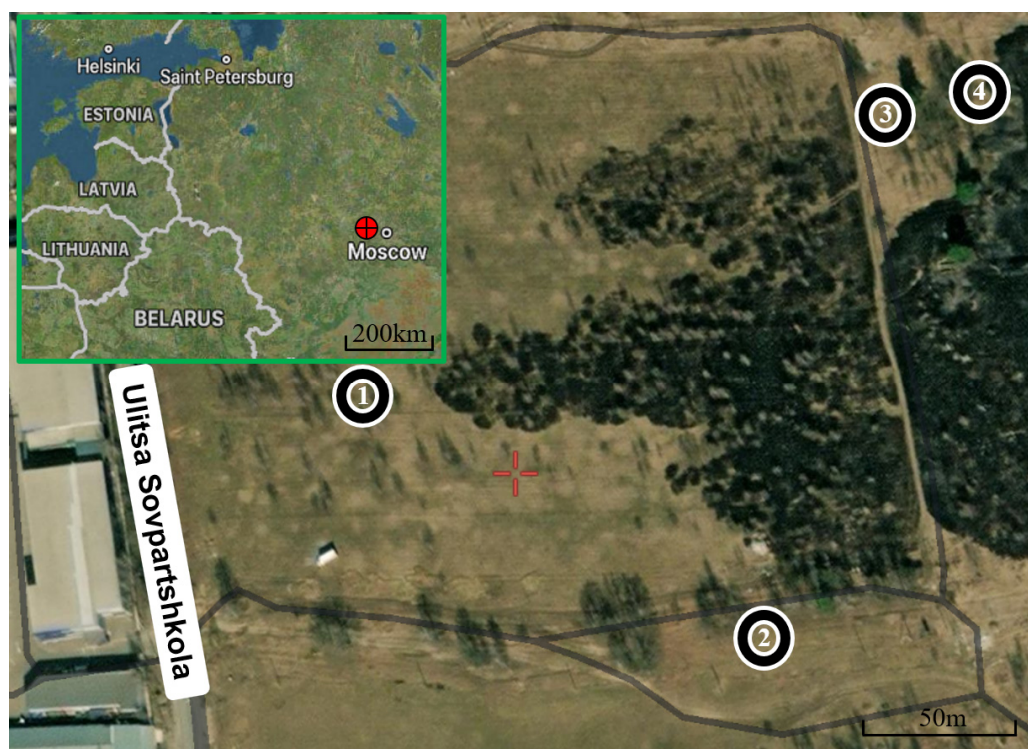


Figure 1. Field experiment site and 4 test points; the experiment site was selected as the edge of Nakhabino in the Moscow region ($55^{\circ}51'44.3''$ N, $37^{\circ}11'21.3''$ E) (Apple map, <https://satellites.pro>, 10 December 2020) [23].

To minimize potential interference and enhance the accuracy of the experimental data, we randomly selected four test points at the experimental site for repeated measurements. The “Kometa-M” multi-gas analyzer (Figure 2), equipped with a methane gas sensor, was used as the measuring device.

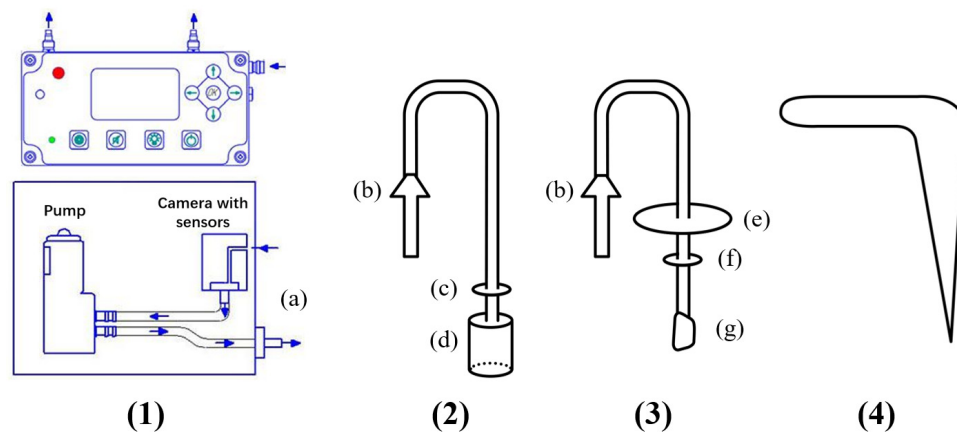


Figure 2. Experimental instruments: (1)—multi-gas analyzer “Kometa-M” (a—pipe coupler, the direction of the arrow is the direction of gas flow), (2)—connector for measuring the concentration of methane on the soil surface (b—dust filter; c—pipe and tank connector; d—iron tank with an opening at the bottom, the other part is sealed); (3)—connector for measuring the methane concentration inside the soil (b—dust filter; e, f—removable sealing auxiliary cover; g—dust filter made of sponge); (4)—20 cm hole punch.

During the experiment, the “Kometa-M” experimental instrument was activated to begin measuring methane concentrations in the air, as shown in Figure 2(1). The device was connected to the setup depicted in Figure 2(2) to measure methane concentrations at the soil surface. To prevent gas leakage, an iron tank (Figure 2(2), d) was inserted approximately 2 cm into the ground. For measuring methane concentrations within the soil, a 20 cm long hole punch was initially used to create access points (Figure 2(4)). These points were then connected to the apparatus in Figure 2(3), where a probe was inserted into the soil to assess the methane levels. During measurements, personnel pressed down on the sealing auxiliary cover (Figure 2(3), e) to minimize gas leakage as much as possible. When measuring the methane concentration in the air, the sensor is positioned 2 m above the surface. For underground measurements, the sensor takes readings 20 cm beneath the surface. The sensor maintains the same resolution and accuracy across different materials, whether measuring airborne or subterranean methane concentrations.

The measurements were conducted using a single Kometa-M instrument, which had been professionally calibrated. Gas analyzers are typically prone to significant measurement errors; therefore, to achieve more accurate data, numerous experiments were conducted in the field. Each measurement lasted 5 min, during which the methane concentration was measured three times in the air, at the soil surface, and within the soil. For greater accuracy, each experiment at each point was performed three times. The device was placed in a gas chamber for calibration. Two points are required to calibrate the channel: the first, involves clean air in the chamber, and the second point uses a gas mixture at a specified concentration supplied to the sensor. The methane resolution is 125 ppm. The accuracy is $\pm 2\%$ FSD at 20 °C (68 °F) with 1 bar pressure and a 2.5% *v/v* methane gas mixture. Since air methane levels can be influenced by concentrations at the soil surface and within, the final stable value from the three readings was recorded for the air measurements. In contrast, for the soil surface and subsurface measurements, the highest of the three readings was taken, as the “Kometa-M” uses a suction pump principle for gas collection. Each of the four measurement points was assessed at three similar spots to ensure that the data collected were both realistic and reliable.

3. Data Results

Through five field experiments (Table 1), the results indicated that during the freezing of the soil surface from, 11 November 2020 to 28 November 2020, there was a significant increase in methane concentrations in the soil, at the soil surface, and in the air. Specifically, the methane concentration in the soil increased by 70% to 370%, at the soil surface by 30% to 87%, and in the air by 19% to 45%. Notably, the methane concentration at test point 2 exceeded the measurement capabilities of the instrument, reaching up to 9000 mg/m³. Concurrently, the concentration of methane at the soil surface and in the air significantly decreased, reaching levels previously unrecorded.

Table 1. Methane concentration during freezing.

Time	Point Number	CH ₄ Concentration, mg/m ³ (in Air)	CH ₄ Concentration, mg/m ³ (on Surface Soil)	CH ₄ Concentration, mg/m ³ (in Soil)	Freezing Thickness on the Surface, cm	Snow Cover Thickness, cm
11 November 2020	1	22	24	72	0	0
	2	20	22	156	0	0
	3	20	22	237	0	0
	4	21	75	54	0	0
28 November 2020	1	28	45	305	3	2
	2	29	31	734	3	4
	3	26	29	413	3	2
	4	25	31	93	3	3
10 December 2020	1	21	27	1356	5	9
	2	23	29	9000	5	10
	3	20	28	6484	4	9
	4	23	25	292	3	7
8 January 2021	1	17	21	884	4	27
	2	20	22	5727	3	31
	3	20	29	5484	1	28
	4	22	27	229	0	24
22 February 2021	1	13	19	537	3	41
	2	25	77	3399	0	80
	3	27	35	2908	0	60
	4	25	32	43	0	55

During the initial frozen state, methane concentrations were 20–30 mg/m³. As the freezing process continued from 10 December 2020 to 8 January 2021, there was a significant reduction in the methane concentration within the soil, ranging from 15% to 36%. Meanwhile, the concentration of methane in the air at the neutralized soil surface remained relatively stable, maintaining levels approximately between 20 and 30 mg/m³.

As the snow cover continued to increase from 8 January 2020 to 22 February 2020, the freezing process of the soil surface gradually weakened, and the soil even completely thawed at test points 2, 3, and 4. Consequently, the methane concentration within the soil continuously decreased, with a reduction ranging from 39% to 81%. Meanwhile, the methane concentration at the soil surface and in the air increased, with increments of 13% to 35% at the soil surface layer and 18% to 250% in the air (Figure 3).

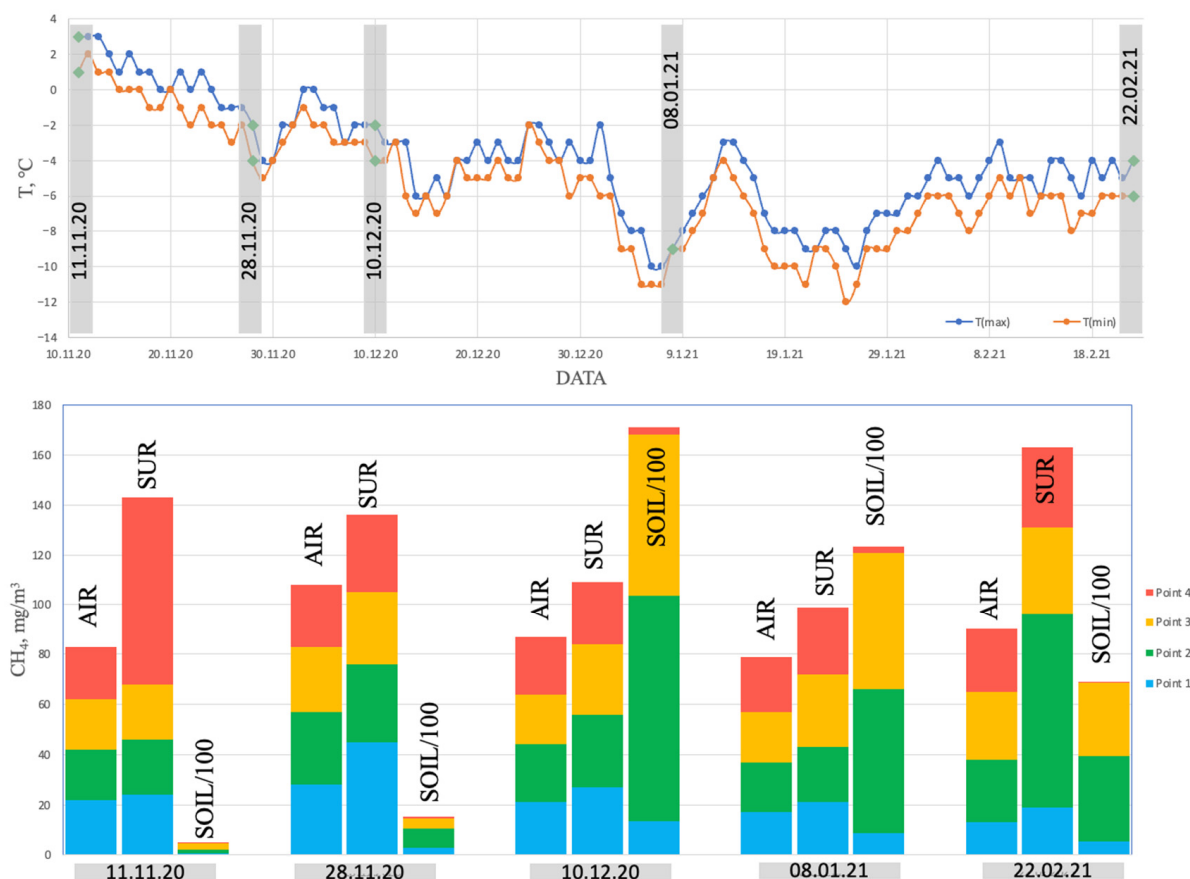


Figure 3. Change in CH₄ content during freezing with temperature in the air, on the surface of the soil, and in the soil (analysis temperature data were taken from the Russian Federal Service for Hydrometeorology and Environmental Monitoring—Roshydromet).

4. Changes in Methane Emissions during the Formation of Frozen Soil

According to the temperature analysis in the Nakhabino area from January 2021 to December 2022, the maximum temperatures (30 °C to 33 °C) were recorded from June to August annually, while the minimum temperatures (−22 °C to −25 °C) occurred from December to February.

The map displays methane concentrations on a 2 km × 2 km grid over land, based on weekly averages, and expressed in parts per billion (ppb). The color scale on the map graphically represents these concentrations. This concentration map draws from data collected by the Tropospheric Monitoring Instrument (TROPOMI), a satellite instrument aboard the Copernicus Sentinel-5 Precursor satellite. The patented Wide-Angle Fabry Perot (WAF-P) imaging spectrometer onboard measures sunlight absorption by methane at a very high spectral resolution. This sensor technology accurately determines methane concentrations for over 200,000 pixels in each image.

In examining the changing trends in the atmospheric methane concentration in Nakhabino from January 2021 to December 2022, it was observed that the methane concentration in the atmosphere increased rapidly around 11 October 2021 and 25 October 2022, as shown in Figure 4. These intervals correspond to the periods when the temperature sharply dropped below 0 °C.

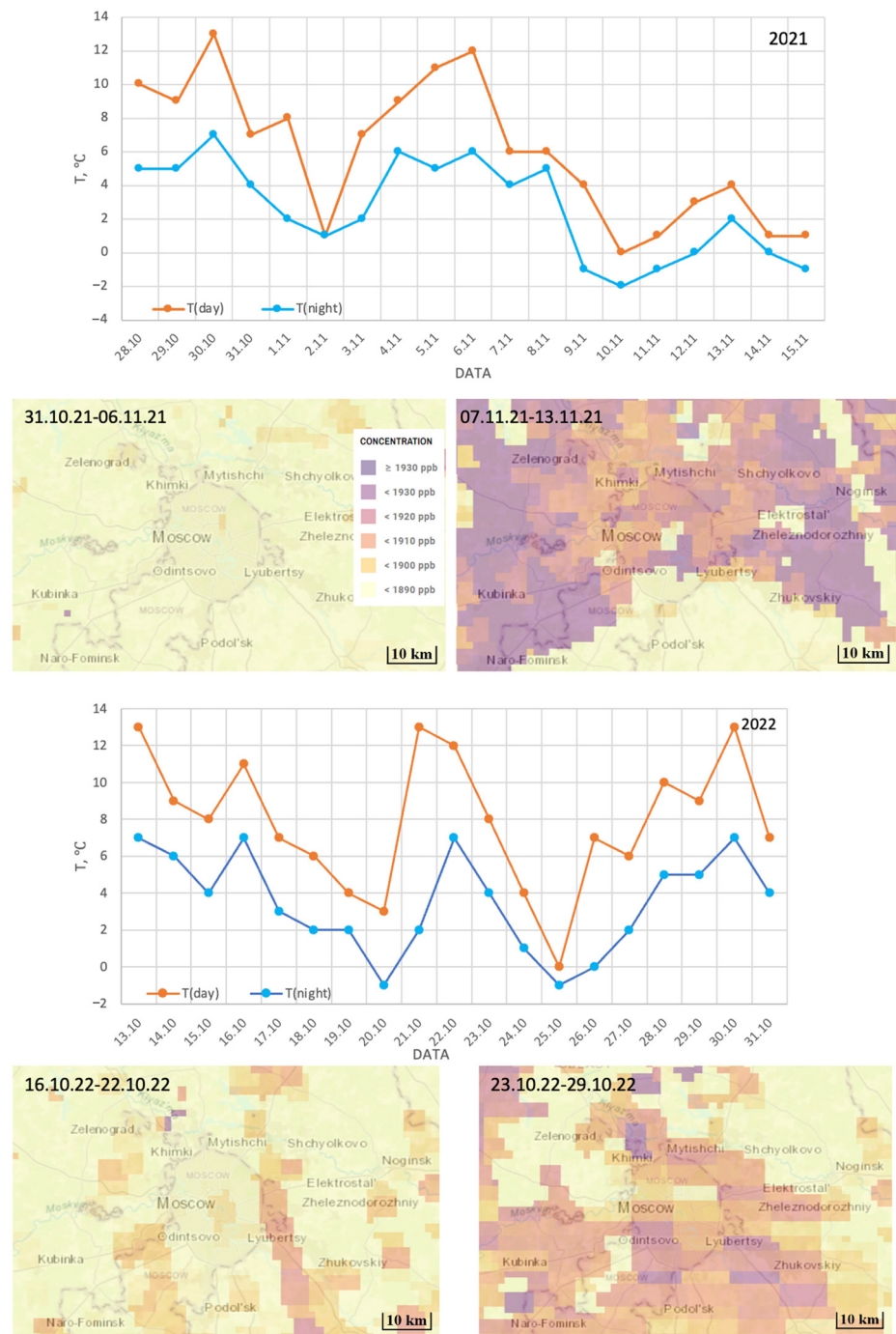


Figure 4. Impact of surface frozen soil layer formation on methane emissions in Nakhabino (data taken from SPECTRA map: <https://spectra-basic.ghgsat.com/> (accessed on 1 July 2024)) [24].

By examining the trends in temperature changes and methane emissions in Nakhabino, it is evident that the release of methane from the soil is influenced by temperature and soil freezing. When temperatures drop below zero degrees Celsius and frozen soil begins to form on the surface, methane emissions increase. This finding aligns with results from field tests. As the surface soil progressively freezes, the methane trapped within the soil is encapsulated by ice, and subsequently, released into the atmosphere.

In the study area, the snow cover thickened as snowfall intensified. The entire Nakhabino region experienced its peak snowfall from the end of January 2022 to the end of February 2022. During this period, methane emissions decreased sharply (Figure 5).

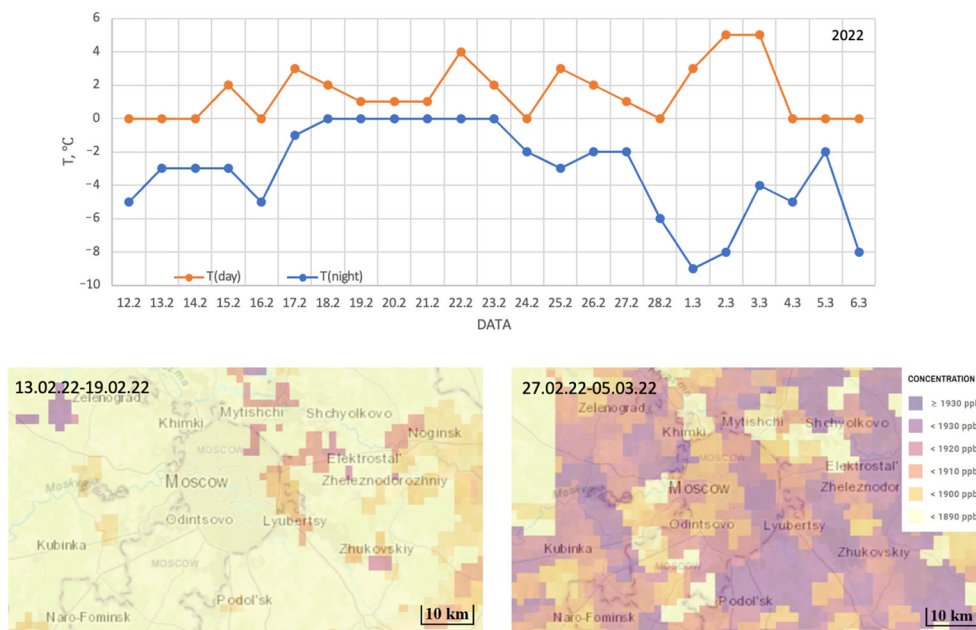


Figure 5. Impact of melting snow cover on methane emissions in 2022 in Nakhabino (data taken from SPECTRA map: <https://spectra-basic.ghgsat.com/> (accessed on 1 July 2024)) [24].

Starting from March 2022, as temperatures gradually rose above zero degrees Celsius by mid-March, the thickness of the snow cover began to decrease. Despite the warming, the frozen soil on the ground surface persisted. Satellite data on snow cover corroborated the findings from field experiments, indicating a sharp increase in methane emissions during this period. These observations highlight the significant influence of snow cover on methane emissions (Figure 6).

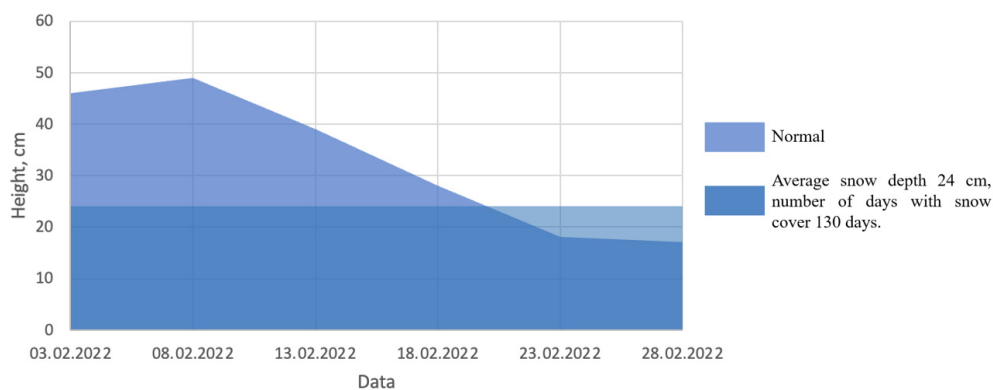


Figure 6. Moscow 2021–2022 snow depth ([https://rp5.ru/%D0%90%D1%80%D1%85%D0%B8%D0%B2_%D0%BF%D0%BE%D0%B3%D0%BE%D0%B4%D1%8B_%D0%B2_%D0%9C%D0%BE%D1%81%D0%BA%D0%B2%D0%B5_\(%D0%92%D0%94%D0%9D%D0%A5\)](https://rp5.ru/%D0%90%D1%80%D1%85%D0%B8%D0%B2_%D0%BF%D0%BE%D0%B3%D0%BE%D0%B4%D1%8B_%D0%B2_%D0%9C%D0%BE%D1%81%D0%BA%D0%B2%D0%B5_(%D0%92%D0%94%D0%9D%D0%A5)) (accessed on 1 July 2024)) [25].

5. Result Analysis

In recent years, increasing attention has been paid to methane emissions under freeze–thaw conditions in permafrost regions, although the factors influencing these emission mechanisms are complex [26–28]. While numerous factors influence methane generation in these regions, this paper specifically excludes the impact of gas generation factors [29–31]. Based on the data obtained, during the initial freezing process of methane (from 11 November 2020 to 28 November 2020), as the soil begins to freeze (to a depth of 3 cm), the glacial soil occupies more underground space, compressing the gas and forcing it to discharge. This leads to increased methane concentrations in the upper soil layer, at the soil surface,

and in the air. When the snow cover is minimal (3–10 cm) and the soil surface freezes further to a depth of 3–5 cm (from 28 November 2020 to 10 December 2020), methane becomes trapped in the soil. This entrapment hinders the escape of gases, resulting in a significant increase in gas concentration within the soil and a corresponding decrease at the soil surface and in the air.

When the snow cover thickness reaches 24–31 cm (from 10 December 2020 to 8 January 2021), the frozen soil layer at the soil surface thins to between 0 and 4 cm. During this period, as the gas concentration within the soil continues to rise and reaches a peak, the internal pressure within the soil also peaks, prompting the gas to be released through various percolation methods, consequently decreasing the methane concentration in the soil [17]. Interestingly, during this process, methane concentrations at test points 1, 2, and 3 displayed a declining trend in both the soil surface and the air, whereas at test point 4, there was a slight increase, which correlates with the degree of freezing at the soil surface. This indicates that the state of freezing at the soil surface is a crucial determinant of gas emissions from the soil, aligning with findings reported by several scholars [19–21] (Figure 7(1)).

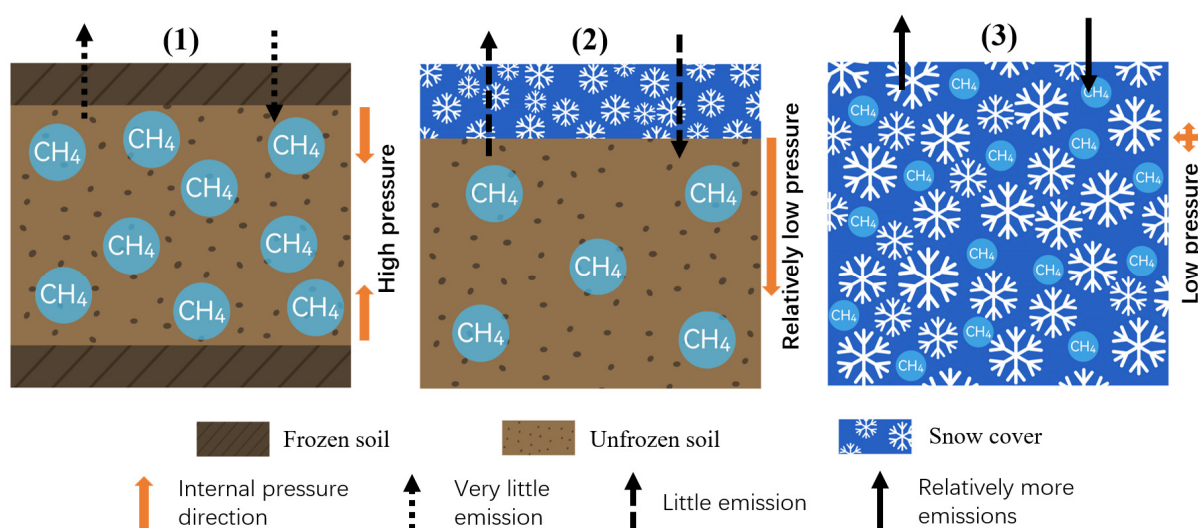


Figure 7. The mechanism of methane emission during freezing (1)—the mechanism of methane emission under the bidirectional compression of the soil surface freezing downward and the subsurface permafrost upward freezing; (2)—the mechanism of methane emission under the condition of snow cover; (3)—transient storage effects and emission mechanisms of snow cover on methane).

When the snow cover reached a thickness of 41–80 cm, the soil surface at test points 2, 3, and 4 exhibited signs of melting between 8 January and 22 February 2020. This condition increased the rate of release of methane, leading to increased concentrations at the soil surface and in the air. This observation suggests that factors mitigating methane emissions extend beyond the formation of permafrost; notably, snow cover also plays a critical role in inhibiting these emissions (Figure 7(2)). During the experiment, it was noted that the porosity of the snow cover not only hindered methane release but also acted as temporary storage for the methane released, a factor that may have been overlooked in previous studies (Figure 7(3)). From these observations, it can be inferred that in permafrost regions, once the snow cover reaches a certain thickness, the upper layers of snow form an ice barrier due to the drop in temperature, while the lower layers of snow serve as a temporary storage for methane emissions from the underlying permafrost. Future strategies for controlling methane emissions and recovering methane could involve slicing through the ice layer to install pipelines between the lower snow cover and the upper permafrost layer for gas extraction. These findings broaden the scope for modeling methane emissions during freeze–thaw cycles [32–34].

6. Conclusions

According to field experiment findings, significant methane releases occur during the autumn and winter transition seasons as the surface soil begins to freeze, a phenomenon that has previously received scant attention in scientific research. The concentrations of methane in the soil, soil surface, and air can reach up to 370%, 87%, and 45%, respectively, of those before freezing. As the snow thickness doubles, the methane concentration in the air can astonishingly increase by 18–250%. Satellite measurement data also corroborate this significant rise. The surface permafrost exhibits a more effective sealing capability than snow cover, capable of containing methane concentrations more than 56 times greater than when the surface soil is unfrozen. Snow cover also plays a crucial role in the gas emission process, able to trap methane at concentrations 20 times higher than before the topsoil freezes, an aspect often overlooked in prior studies. Furthermore, the porosity and permeability of the snow cover contribute not only to its barrier effect but also enable it to serve as a storage medium for gases, another facet that has been underexplored. The effectiveness of snow cover with varying structures in gas barrier and storage roles warrants separate, detailed experimental and analytical work in future studies. Such research will enhance our understanding of methane emission mechanisms during the freezing and thawing cycles and will be invaluable in devising strategies to mitigate methane emissions in permafrost regions.

Author Contributions: Conceptualization, A.V.B. and V.G.C.; methodology, A.V.S.; software, C.L. and B.Z.; validation, C.L., A.V.B. and A.V.S.; formal analysis, C.L., B.Z., A.V.B. and V.G.C.; investigation, C.L. and A.V.B.; resources, A.V.B. and A.V.S.; data curation, C.L.; writing—original draft preparation, C.L.; writing—review and editing, C.L., A.V.B. and V.G.C.; visualization, C.L.; supervision, A.V.B. and A.V.S.; project administration, A.V.B.; funding acquisition, A.V.B. All authors have read and agreed to the published version of the manuscript.

Funding: This research received no external funding.

Institutional Review Board Statement: Not applicable.

Informed Consent Statement: Not applicable.

Data Availability Statement: The authors confirm that the data supporting the findings of this study are available within the article.

Acknowledgments: The authors thank the China Scholarship Council (no. 202008090312) for supporting this work.

Conflicts of Interest: The authors declare no conflict of interest. The funding sponsors had no role in the design of the study; in the collection, analyses, or interpretation of data; in the writing of the manuscript, and in the decision to publish the results.

References

1. Pachauri, R.K.; Allen, M.R.; Barros, V.R.; Broome, J.; Cramer, W.; Christ, R.; Church, J.A.; Clarke, L.; Dahe, Q.; Dasgupta, P.; et al. *Climate Change 2014: Synthesis Report. Contribution of Working Groups I, II and III to the Fifth Assessment Report of the Intergovernmental Panel on Climate Change*; IPCC: Geneva, Switzerland, 2015; 151p.
2. Hugelius, G.; Strauss, J.; Zubrzycki, S.; Harden, J.W.; Schuur, E.A.G.; Ping, C.-L.; Schirrmeister, L.; Grosse, G.; Michaelson, G.J.; Koven, C.D.; et al. Estimated stocks of circumpolar permafrost carbon with quantified uncertainty ranges and identified data gaps. *Biogeosciences* **2014**, *11*, 6573–6593. [[CrossRef](#)]
3. Jobbágy, E.G.; Jackson, R.B. The vertical distribution of soil organic carbon and its relation to climate and vegetation. *Ecol. Appl.* **2000**, *10*, 423–436. [[CrossRef](#)]
4. Comyn-Platt, E.; Hayman, G.; Huntingford, C.; Chadburn, S.E.; Burke, E.J.; Harper, A.B.; Collins, W.J.; Webber, C.P.; Powell, T.; Cox, P.M.; et al. Carbon Budgets for 1.5 and 2 °C Targets Lowered by Natural Wetland and Permafrost Feedbacks. *Nat. Geosci.* **2018**, *11*, 568–573. [[CrossRef](#)]
5. Randers, J.; Goluke, U. An Earth System Model Shows Self-Sustained Thawing of Permafrost Even If All Man-Made GHG Emissions Stop in 2020. *Sci. Rep.* **2020**, *10*, 18456. [[CrossRef](#)]

6. Strauss, J.; Schirrmeyer, L.; Grosse, G.; Wetterich, S.; Ulrich, M.; Herzsich, U.; Hubberten, H.-W. The deep permafrost carbon pool of the Yedoma region in Siberia and Alaska. *Geophys. Res. Lett.* **2013**, *40*, 6165–6170. [[CrossRef](#)]
7. Strauss, J.; Schirrmeyer, L.; Grosse, G.; Fortier, D.; Hugelius, G.; Knoblauch, C.; Romanovsky, V.; Schädel, C.; Schneider von Deimling, T.; Schuur, E.A.G.; et al. Deep Yedoma permafrost: A synthesis of depositional characteristics and carbon vulnerability. *Earth-Sci. Rev.* **2017**, *172*, 75–86. [[CrossRef](#)]
8. Schuur, E.A.G.; McGuire, A.D.; Schädel, C.; Grosse, G.; Harden, J.W.; Hayes, D.J.; Hugelius, G.; Koven, C.D.; Kuhry, P.; Lawrence, D.M.; et al. Climate change and the permafrost carbon feedback. *Nature* **2015**, *520*, 171–179. [[CrossRef](#)]
9. Tarnocai, C.; Canadell, J.G.; Schuur, E.A.G.; Kuhry, P.; Mazhitova, G.; Zimov, S.A. Soil organic carbon pools in the northern circumpolar permafrost region *Glob. Biogeochem. Cycle* **2009**, *23*, GB2023. [[CrossRef](#)]
10. Romanovsky, V.E.; Drozdov, D.S.; Oberman, N.G.; Malkova, G.V.; Kholodov, A.L.; Marchenko, S.S.; Moskalenko, N.G.; Sergeev, D.O.; Ukraintseva, N.G.; Abramov, A.A.; et al. Thermal state of permafrost in Russia. *Permafrost. Periglac. Process.* **2010**, *21*, 136–155. [[CrossRef](#)]
11. Zimov, S.A.; Schuur, E.A.G.; Chapin, F.S. Permafrost and the global carbon budget. *Science* **2006**, *312*, 1612–1613. [[CrossRef](#)]
12. Zhang, T.; Barry, R.G.; Knowles, K.; Heginbottom, J.A.; Brown, J. Statistics and characteristics of permafrost and ground-ice distribution in the Northern Hemisphere. *Polar Geogr.* **1999**, *23*, 132–154. [[CrossRef](#)]
13. Lawrence, D.M.; Slater, A.G. A projection of severe near-surface permafrost degradation during the 21st century. *Geophys. Res. Lett.* **2005**, *32*, L24401. [[CrossRef](#)]
14. Turetsky, M.R.; Abbott, B.W.; Jones, M.C.; Anthony, K.W.; Olefeldt, D.; Schuur, E.A.G.; Koven, C.; McGuire, A.D.; Grosse, G.; Kuhry, P.; et al. Permafrost Collapse Is Accelerating Carbon Release. *Nature* **2019**, *569*, 32–34. [[CrossRef](#)] [[PubMed](#)]
15. Li, T.; Chen, Y.-Z.; Han, L.-J.; Cheng, L.-H.; Lv, Y.-H.; Fu, B.-J.; Feng, X.-M.; Wu, X. Shortened duration and reduced area of frozen soil in the Northern Hemisphere. *Innovation* **2021**, *2*, 100146. [[CrossRef](#)] [[PubMed](#)]
16. Bao, T.; Xu, X.; Jia, G.; Billesbach, D.P.; Sullivan, R.C. Much stronger tundra methane emissions during autumn-freeze than spring-thaw. *Glob. Change Biol.* **2021**, *27*, 376–387. [[CrossRef](#)]
17. Mastepanov, M.; Sigsgaard, C.; Dlugokencky, E.J.; Houweling, S.; Ström, L.; Tamstorf, M.P.; Christensen, T.R. Large tundra methane burst during onset of freezing. *Nature* **2008**, *456*, 628–630. [[CrossRef](#)]
18. Yang, W.; Song, C.; Zhang, J. Dynamics of Methane Emissions from a Freshwater Marsh of Northeast China. *Sci. Total Environ.* **2006**, *371*, 286–292. [[CrossRef](#)]
19. Pirk, N.; Santos, T.; Gustafson, C.; Johansson, A.J.; Tufvesson, F.; Parmentier, F.-J.W.; Mastepanov, M.; Christensen, T.R. Methane emission bursts from permafrost environments during autumn freeze-in: New insights from ground-penetrating radar. *Geophys. Res. Lett.* **2015**, *42*, 6732–6738. [[CrossRef](#)]
20. Wille, C.; Kutzbach, L.; Sachs, T.; Wagner, D.; Pfeiffer, E.M. Methane emission from Siberian arctic polygonal tundra: Eddy covariance measurements and modeling. *Glob. Change Biol.* **2008**, *14*, 1395–1408. [[CrossRef](#)]
21. Tagesson, T.; Mölder, M.; Mastepanov, M.; Sigsgaard, C.; Tamstorf, M.P.; Lund, M.; Falk, J.M.; Lindroth, A.; Christensen, T.R.; Ström, L. Land-atmosphere exchange of methane from soil thawing to soil freezing in a high-Arctic wet tundra ecosystem. *Glob. Change Biol.* **2012**, *18*, 1928–1940. [[CrossRef](#)]
22. Belaya, N.I.; Dubinin, E.P.; Ushakov, S.A. Geological structure of the Moscow region. In *Geological Practices: M*; Publishing House of Moscow State University: Moscow, Russia, 2001.
23. Apple Map. Available online: <https://satellites.pro> (accessed on 15 March 2024).
24. Data Taken from SPECTRA Map. Available online: <https://spectra-basic.ghgsat.com> (accessed on 20 February 2024).
25. Weather Archive in Moscow (VDNH). Available online: [https://rp5.ru/%D0%90%D1%80%D1%85%D0%B8%D0%B2_%D0%BF%D0%BE%D0%B3%D0%BE%D0%B4%D1%8B_%D0%B2_%D0%9C%D0%BE%D1%81%D0%BA%D0%B2%D0%B5_\(%D0%92%D0%94%D0%9D%D0%A5\)](https://rp5.ru/%D0%90%D1%80%D1%85%D0%B8%D0%B2_%D0%BF%D0%BE%D0%B3%D0%BE%D0%B4%D1%8B_%D0%B2_%D0%9C%D0%BE%D1%81%D0%BA%D0%B2%D0%B5_(%D0%92%D0%94%D0%9D%D0%A5)) (accessed on 25 February 2024).
26. Zona, D.; Gioli, B.; Commane, R.; Lindaas, J.; Wofsy, S.C.; Miller, C.E.; Chang, R.Y.W. Cold season emissions dominate the Arctic tundra methane budget. *Proc. Natl. Acad. Sci. USA* **2016**, *113*, 40–45. [[CrossRef](#)] [[PubMed](#)]
27. Zheng, J.; RoyChowdhury, T.; Yang, Z.; Gu, B.; Wullschlegel, S.D.; Graham, D.E. Impacts of temperature and soil characteristics on methane production and oxidation in Arctic tundra. *Biogeosciences* **2018**, *15*, 6621–6635. [[CrossRef](#)]
28. Hinkel, K.M.; Paetzold, F.; Nelson, F.E.; Bockheim, J.G. Patterns of soil temperature and moisture in the active layer and upper permafrost at Barrow, Alaska: 1993–1999. *Glob. Planet. Change* **2001**, *29*, 293–309. [[CrossRef](#)]
29. Blodau, C. Carbon cycling in peatlands—A review of processes and controls. *Environ. Rev.* **2002**, *10*, 111–134. [[CrossRef](#)]
30. Comas, X.; Slater, L.; Reeve, A. Seasonal geophysical monitoring of biogenic gases in a northern peatland: Implications for temporal and spatial variability in free phase gas production rates. *J. Geophys. Res. Biogeosci.* **2008**, *113*, G01012. [[CrossRef](#)]
31. Moore, T.R.; Dalva, M. Methane and carbon dioxide exchange potentials of peat soils in aerobic and anaerobic laboratory incubations. *Soil Biol. Biochem.* **1997**, *29*, 1157–1164. [[CrossRef](#)]
32. Treat, C.C.; Bloom, A.A.; Marushchak, M.E. Nongrowing season methane emissions—A significant component of annual emissions across northern ecosystems. *Glob. Change Biol.* **2018**, *24*, 3331–3343. [[CrossRef](#)]

33. Kirschke, S.; Bousquet, P.; Ciais, P.; Saunoy, M.; Canadell, J.G.; Dlugokencky, E.J.; Bergamaschi, P.; Bergmann, D.; Blake, D.R.; Bruhwiler, L.; et al. Three decades of global methane sources and sinks. *Nat. Geosci.* **2013**, *6*, 813–823. [[CrossRef](#)]
34. Mastepanov, M.; Sigsgaard, C.; Tagesson, T.; Ström, L.; Tamstorf, M.P.; Lund, M.; Christensen, T.R. Revisiting factors controlling methane emissions from high-Arctic tundra. *Biogeosciences* **2013**, *10*, 5139–5158. [[CrossRef](#)]

Disclaimer/Publisher’s Note: The statements, opinions and data contained in all publications are solely those of the individual author(s) and contributor(s) and not of MDPI and/or the editor(s). MDPI and/or the editor(s) disclaim responsibility for any injury to people or property resulting from any ideas, methods, instructions or products referred to in the content.